Atmospheric Research 278 (2022) 106360

Contents lists available at ScienceDirect

Atmospheric Research

journal homepage: www.elsevier.com/locate/atmosres

Secondary organic carbon in different atmospheric environments of a continental region and seasons

Imre Salma [a,*], Péter Tibor Varga [a], Anikó Vasanits [a], Attila Machon [b]

[a] Institute of Chemistry, Eötvös Loránd University, Budapest, Hungary
[b] Air Quality Reference Center, Hungarian Meteorological Service, Budapest, Hungary

ARTICLE INFO

Keywords:
Organic carbon
Secondary organic aerosol
EC tracer method
High EC edge approximation

ABSTRACT

Secondary organic carbon (SOC) was derived using elemental carbon (EC) tracer method for primary organic carbon (OC) in daily aerosol samples collected in the regional background environment, suburban area, and central part of Budapest in each season. The estimation approaches of the OC/EC ratio for the major emission sources required for the tracer method were discussed, and the high EC edge approach was adopted separately for each location and season. The annual mean SOC concentrations in the environments listed were 1.16, 1.51 and 1.42 μg m^{-3}, respectively. They were interpreted together with the $PM_{2.5}$ mass, OC, EC, water-soluble OC (WSOC), levoglucosan (LVG) and meteorological variables. The annual mean contributions of SOC to OC were 45% at all sampling sites. However, they showed substantial seasonal variation at each location. The shares were the smallest (<≈30%) in winter, whereas they prevailed in summer (in the regional background, this even reached 66%). The secondary organic aerosol (obtained by multiplying the SOC concentrations by the organic mass-to-OC correction factor) made up roughly 25% of the $PM_{2.5}$ mass except for winter, when it was 10%. Obvious associations of the SOC on the one side and $PM_{2.5}$ mass, OC and WSOC on the other side were identified as joint relationships for all seasons. The SOC correlated with LVG only in winter when the relative intensity of biomass burning is the highest, and with O_3 only in spring and summer, when the role of photochemistry is considerable. Elevations in $PM_{2.5}$ mass, OC and WSOC concentrations on a daily scale were related to the enhancement of SOC concentration by factors of 0.14, 0.4 and 0.6, respectively, while higher LVG levels in winter enlarged the SOC 3-times. There was a relationship between the SOC and OC from fossil fuel combustion over all seasons, whereas the dependency between the SOC and OC from biomass burning could be established only in winter, and between the SOC and OC from biogenic sources apart from winter. The results and conclusions have importance for the health consequences of SOC in cities and rural areas over the whole Carpathian Basin.

1. Introduction and objectives

The role of aerosols in the Earth system and their effects on human health, climate, the environment, and ecological integrity are important from many aspects from local to global spatial scales (e.g., Carslaw et al., 2010; Lelieveld et al., 2015 and references therein). One of their relevant size fractions contains particles with an equivalent diameter of <2.5 μm ($PM_{2.5}$), which is often characterised by its total mass and chemical composition. Its largest part consists of carbonaceous particles (Kanakidou et al., 2005; Zhang et al., 2007; Jimenez et al., 2009). They are mainly generated by fossil fuel (FF) combustion, biomass burning (BB) and biogenic sources. Despite its abundance and potential implications, the carbonaceous matter remains poorly understood mainly due to its chemical complexity (Fuzzi et al., 2015; Saleh et al., 2015; Nozière et al., 2015; Glasius and Goldstein, 2016).

The fine-fraction carbonaceous particles are basically composed of soot and organic compounds. The former can be expressed by elemental carbon (EC), while the latter – which make up the organic matter, OM – is often quantified by an aggregate measure, namely organic carbon (OC). The OC can be separated into further groups, for instance, brown carbon, secondary organic carbon (SOC), water-soluble organic carbon (WSOC) or carbon in atmospheric humic-like substances (HULIS). They all express important properties and processes of carbonaceous species or contain valuable information on their sources. Some further relevant

* Corresponding author.
E-mail address: salma.imre@ttk.elte.hu (I. Salma).

https://doi.org/10.1016/j.atmosres.2022.106360
Received 24 February 2022; Received in revised form 20 June 2022; Accepted 21 July 2022
Available online 27 July 2022

chemical constituents such as levoglucosan (LVG), polycyclic aromatic hydrocarbons and phthalates are determined at molecular level (Hays et al., 2003; Nozière et al., 2015; Alves et al., 2016). Levoglucosan can be utilized as tracers for BB in source apportionment studies. The other two chemical groups can be applied to assess some specific health impacts (e.g. carcinogenic effects and endocrine disruption, respectively) of the carbonaceous matter.

Of these groups, the SOC is an important and useful quantity (Griffin et al., 2002; Hallquist et al., 2009; McFiggans et al., 2019). The related chemical species are formed in the atmosphere by oxidizing volatile organic compounds (VOCs) in chemical reactions or enter the atmosphere as organic vapours. They can finally condense on the available particles or molecular clusters, so they can be partitioned between particulate and vapour phases (Fuzzi et al., 2015). It is estimated that approximately 85%–90% of SOC is produced by oxidation of biogenic emissions on the global scale, particularly in terrestrial ecosystems (Kanakidou et al., 2005; Tsigaridis and Kanakidou, 2007; Guenther et al., 2012). Of them, isoprene and monoterpenes have been identified as major aerosol precursors, and their low-volatility oxidation products have been shown to play a role (Claeys et al., 2004; Ehn et al., 2014).The situation in cities and industrial areas can be different from this (Hoyle et al., 2011; Timonen et al., 2017; McFiggans et al., 2019; Via et al., 2021). The nonlinearity in their formation and the involved feedback mechanisms make the study of secondary organic aerosol (SOA) challenging. It has been associated with increased health risk (Pandis et al., 2016; Nault et al., 2021), oxidative potential (Daellenbach et al., 2020) and hygroscopic or water-activation properties of particles (Swietlicki et al., 2008; Wang et al., 2021). The knowledge on their properties is required to design effective strategies for improving air quality as well. In contrast, the primary organic aerosol (POA, expressed collectively by primary organic carbon, POC) is assumed to be nonvolatile. It has been shown, however, that a substantial fraction of the freshly produced POA evaporates after emission (Robinson et al., 2007). In addition, both primary and secondary carbonaceous particles can continue to change due to further atmospheric processes called chemical aging. This indicates the relationships between SOA and POA.

Atmospheric SOC (and POC) can be estimated by EC tracer method using measured ambient OC and EC concentrations (Turpin and Huntzicker, 1995). Another important possibility is the aerosol mass spectrometry (AMS) that can determine several organic fractions with high time and size resolutions (Jimenez et al., 2003; Allan et al., 2004; Aiken et al., 2008). Multistatistical methods applied to these or other offline data sets can separate the OC into several chemical groups, which show direct or indirect correspondence with SOC and POC (e.g., Tang et al., 2018; Via et al., 2021). Some key organic species (SOA tracers) have also been identified as characteristics of SOC and can be used to its source apportionment (e.g., Lanzafame et al., 2021). The EC tracer method is beneficial from the point of view that it does demand neither very sophisticated techniques nor very extensive data sets nor many samples, and that the required analytical data are ordinarily readily available in those experiments.

Several studies have been conducted in the Carpathian Basin including its major city of Budapest dealing with carbonaceous aerosol (e.g., Salma et al., 2004, 2007, 2017; Gelencsér et al., 2007; Maenhaut et al., 2008). However, there is still a large gap in our knowledge regarding the SOC, and its spatial and temporal characteristics. Recently, aerosol samples were collected in parallel with each other in the regional background environment, suburban area, and city centre of Budapest in each season for 1-year-long time interval, and they were analysed for various chemical constituents. The analytical results were already utilized to apportion the total carbon (TC=OC + EC) into EC and OC from FF combustion and BB, and into OC from biogenic sources by a coupled radiocarbon-LVG marker method (Salma et al., 2020). Here we focus on the SOC. The major objectives of this paper are to present and discuss the EC tracer method with an advanced adaptation of the high EC edge approach, to estimate and debate the derived SOC concentrations and particularly, their shares in the OC, and to assess and interpret the relationships among SOC and some other aerosol constituents and environmental variables. The results and conclusions contribute to improved methodology of the EC tracer method, facilitate our better understanding the SOA properties, and represent the first systematic information of this type in several connected atmospheric environments in the Carpathian Basin over 1 year.

2. Methods

2.1. Samplings, analyses, and online measurements

The aerosol samples were collected at three sites which express different atmospheric environments in the Carpathian Basin. This is the largest orogenic basin in Europe and represents a considerable territory of its continental part (Salma et al., 2020). The sampling in the regional background environment was performed at the K-puszta station (N 46° 57′ 56″, E 19° 32′ 42″, 125 m above sea level, a.s.l.). It is part of the EMEP network and represents the main plain part of the basin. Budapest with 2.3 million inhabitants in the metropolitan area is its largest city. The suburban sampling site was in an open area in residential Budapest at the Marczell György Main Observatory (N 47° 25′ 46“, E 19°10’ 54”, 138 m a.s.l.) of the Hungarian Meteorological Service. The collections in the city centre were realised at the Budapest platform for Aerosol Research and Training (BpART) Laboratory (N 47° 28′ 30″, E 19° 03′ 45″, 115 m a.s.l.). This represents an average atmosphere of the city centre (Salma et al., 2016). The actual selection of the sampling sites realises a gradual transition from the central part of a large city to its regional (rural) background environment.

Three identical high-volume sampling devices equipped with $PM_{2.5}$ inlets (DHA-80, Digitel, Switzerland) were deployed at the locations. The collection substrates were quartz fibre filters with a diameter of 150 mm (QR-100, Advantec, Japan). The filters were pre-heated at 500 °C for 24 h. Daily aerosol samples were collected starting at 00:00 local time. The samples were collected in parallel with each other over consecutive days in October 2017 (autumn), January 2018 (winter), April 2018 (spring) and July 2018 (summer). Details on the samplings and filters are summarised in Table S1 in the Supplement. The sampled air volumes were typically 720 m^3. One field blank sample was also taken at each location and month. The exposed filters were stored in a freezer.

Particulate matter mass was determined by gravimetry (Cubis MSA225S-000-DA, Sartorius, Germany, sensitivity of 10 μg) after pre-equilibrating the samples at a temperature of 19–21 °C and relative humidity of 45%–50% for at least 48 h. The measured mass data for the exposed filters were corrected for the field blank values. The PM mass data were usually above the limit of quantitation (LOQ), which was below 1 μg m^{-3}.

Filter punches were analysed by thermal-optical transmission (TOT) method using a laboratory OC/EC analyser (Sunset Laboratory, USA) adopting the EUSAAR-2 thermal protocol (Cavalli et al., 2010). The OC data for the exposed filters were corrected for the field blank values, while the EC on the blank filters was negligible (Salma et al., 2020). All OC and EC data were above the LOQ, which was 0.38 and 0.04 μg m^{-3}, respectively.

Filter sections were extracted in deionized water, and the filtered extracts were analysed for WSOC by a Vario TOC cube analyser (Elementar, Germany). The measured WSOC data for the exposed filters were corrected for the field blank values. All measured WSOC data were above the LOQ, which was 0.08 μg m^{-3}.

Filter pieces were analysed for LVG by gas chromatography–mass spectrometry (Varian 4000, USA) after trimethylsilylation (Blumberger et al., 2019; Salma et al., 2020). The LVG data for the exposed filters were corrected for blanks. All LVG data were above the LOQ, which was 1.2 ng m^{-3}.

Air pollutants of NO/NO_x, CO and O_3 were obtained from regular

stations of the National Air Quality Network. For the regional background and suburban area, they were measured directly at the sampling sites, while for the city centre, the pollutants were recorded in 4.5 km in the upwind prevailing direction from the sampling site. The concentrations are measured by chemiluminescence (Thermo 42C), IR absorption (Thermo 48i) and UV absorption (Ysselbach 49C) methods, respectively and were retrieved with a time resolution of 1 h.

Local meteorological data including air temperature (T), relative humidity (RH), wind speed (WS) and global solar radiation (GRad) were acquired by standardised and calibrated meteorological methods (humidity and temperature probes with anemometer: HD52.3D17, Delta OHM, Italy or Vaisala HMP45D and Vaisala WAV15A, Finland; pyranometers: CMP3 or CMP11, Kipp and Zonen, The Netherlands) on sites with a time resolution of 10 min.

Further details on the sampling locations, collection campaigns and analyses were described previously (Salma et al., 2020).

2.2. EC tracer method

Secondary organic carbon was estimated using EC as tracer for POC emissions (Turpin and Huntzicker, 1995) as:

$$\mathrm{SOC} = \mathrm{OC} - \mathrm{POC} = \mathrm{OC} - \left(\frac{\mathrm{OC}}{\mathrm{EC}}\right)_{\mathrm{P}} \times \mathrm{EC} - a, \quad (1)$$

where OC and EC are measured ambient concentrations, $(\mathrm{OC/EC})_{\mathrm{P}}$ is the OC-to-EC ratio for the major emission (combustion) sources and a is intercept. It is assumed that POC and EC have the same major primary sources, and that there is a constant $(\mathrm{OC/EC})_{\mathrm{P}}$ ratio for them during the samplings. The method also assumes that POC is nonvolatile and nonreactive. The intercept a is discussed in detail in Sect. 3.1. Estimation of the ratio is crucial to the method, and several adaptations were proposed to perform this.

A common approach is to isolate sampling intervals for an area and time of interest during which a high primary contribution to OC is expected and to calculate the mean OC/EC ratio for these selected intervals from measured atmospheric concentrations (Turpin and Huntzicker, 1995; Lim and Turpin, 2002; Pio et al., 2011). The selection can be done by including only the lowest observed OC/EC ratios into the averaging that are assumed to represent pure primary aerosol (Castro et al., 1999), or by excluding the data from the averaging for which an intense SOC formation can be identified (Strader et al., 1999; Cabada et al., 2004). The two selection attitudes can be performed jointly (Salma et al., 2004). Secondary organic aerosol formation is often suppressed when photochemical activity is low (i.e., under low GRad and at low O_3 levels) and in rain. Large contributions of POC can be associated with high levels of pollutants co-emitted with POC such as NO and CO. In some other studies, road tunnel measurements were applied directly to estimate the $(\mathrm{OC/EC})_{\mathrm{P}}$ although the dilution processes and their consequences could be different in tunnels and ambient air (Lonati et al., 2005). This approach is sometimes called traditional EC tracer method since it has been prevalent in the literature.

Another approach is to select the highest primary contributions by choosing those EC/OC ratios that are considerably above the mean EC/OC value (e.g., by twice the SD or above a certain percentile; Day et al., 2015; Kaskaoutis et al., 2020). This is realised jointly by investigating the scatter plot of OC and EC concentrations and by fitting a linear regression to the selected data pairs. The major difference from the traditional approach is that the selected OC and EC data pairs are fitted with a regression line, and its slope (b) yields the requested ratio: $(\mathrm{OC/EC})_{\mathrm{P}} = b$. This treatment is sometimes called the high EC edge approach.

The selecting criteria in both approaches can sometimes be made more objective and traceable using the minimum R^2 method (Millet et al., 2005; Wu and Yu, 2016). This assumes that EC is independent of SOC and, therefore, the $(\mathrm{OC/EC})_{\mathrm{P}}$ should be the ratio resulting in minimum correlation between the estimated SOC and measured EC. Its weakness is that a significant part of SOC can be generated by photooxidation of VOCs coemitted with EC (Wu et al., 2019), and, therefore, this selection method can underestimate the SOC (Kaskaoutis et al., 2020).

The traditional approach seems to result in reliable estimates in cases of low SOC contributions and if POC emissions are evenly spread and temporally constant (Castro et al., 1999; Pio et al., 2011; Zhang et al., 2005). Both approaches were critically evaluated with respect to the simulated concentrations obtained by the chemical transport model PMCAMx as well (Day et al., 2015). It was concluded that the high EC edge approach performed better than the traditional treatment for both SOC and POC, particularly for low POC/OC ratios. At the same time, the POC was advised to be interpreted with caution, since it incorporates fresh POC and SOC from POC evaporation and oxidation and from background OC as well. Some other studies indicated that the difference in the $(\mathrm{OC/EC})_{\mathrm{P}}$ ratios estimated by these two approaches decreases with SOC contribution (Wu and Yu, 2016; Kaskaoutis et al., 2020).

It is important to be aware that all approaches discussed above use the EC tracer method framework and they just estimate the $(\mathrm{OC/EC})_{\mathrm{P}}$ ratio in a different manner. Therefore, their main limitation is also common, namely that the actual $(\mathrm{OC/EC})_{\mathrm{P}}$ ratios can actually vary spatially and temporally, e.g., by local source types such as road vehicles, fireplaces, and cooking, and by meteorology and season (Wu et al., 2019). In addition, POC emissions from non-combustion sources, such as biogenic emissions and soil suspension, which both can partly contribute to the $PM_{2.5}$ size fraction, are not accounted for by the methods. As a result, the data derived by any combination of the approaches are subject to larger uncertainties which are inherent to the EC tracer method framework (Pio et al., 2011; Grivas et al., 2019; Wu et al., 2019).

3. Results and discussion

Atmospheric concentrations, meteorological properties and their relationships were presented previously (Salma et al., 2020). It is just noted here that the carbonaceous species made up from 32% to 39% of the $PM_{2.5}$ mass with a modest seasonal variation and with a slightly increasing tendency from the regional background to the city centre.

3.1. OC/EC ratios for primary sources

The time series of the OC/EC ratios showed irregular variations. Their ranges and means with SDs in the regional background, suburban area and city centre were from 5.7 to 29 and 11.9 ± 5.0, from 2.8 to 14.1 and 7.0 ± 2.4, and from 2.5 to 8.6 and 5.6 ± 1.9, respectively. They indicate a decreasing tendency in the order of the sites and are in line with our previous studies and general knowledge on source types of the carbonaceous matter. Kerbside sites, road canyons and tunnels typically yield OC/EC values around 2 (Salma et al., 2004). For primary aerosol from diesel engines, a ratio down to 1.1 was obtained (Kleeman et al., 2000). The ratios for BB emissions are usually larger than for FF combustion, and also show a wider range (4–16) depending on the burning material, its moisture content, (flaming or smouldering) fire conditions and aerosol aging (Pio et al., 2011; Vicente and Alves, 2018).

Estimation of the $(\mathrm{OC/EC})_{\mathrm{P}}$ ratio was essentially accomplished using the high EC edge approach (Sect. 2.2). Based on the features and arguments in the previous paragraph, season-specific $(\mathrm{OC/EC})_{\mathrm{P}}$ ratios at each location were derived. Those OC and EC data were selected for the calculations for which the OC/EC ratios were smaller than the lower quartile of the ratios. The selected OC and EC data pairs were double checked by considering the corresponding concentration levels of NO, CO and O_3 and by meteorological properties such as GRad and WS. Some OC and EC data pairs were added to the selection for which the concentrations of these pollutants and meteorological properties were larger than the upper quartile (for O_3 and WS, smaller than the lower quartile) of their ranges if there was a need to improve the regression

statistics. The original selection was extended only in few cases. The days with considerable precipitation were disregarded. The selected data pairs were finally fitted by a linear regression line considering the uncertainty of the concentration data using the instrumental weighting method.

The scatter plots of the measured OC and EC concentrations with the regression lines fitted to the selected data pairs for the suburban area in all seasons are shown in Fig. 1 as examples. The data sets for the other sampling locations were like them. The selected data pairs were reasonably scattered around the regression line, and almost all unselected data pairs were above it. They indicate that the regression lines derived represent the major primary sources and are sensible approximation to reality.

The slope and intercept of the regression lines for all sampling sites and seasons are summarised in Table 1. It is seen that the slopes – i.e., the $(OC/EC)_P$ ratios – changed substantially for different seasons at a particular location. There is a tendency for smaller slopes in spring and

Table 1
Intercept (a, in μg m^{-3}) and slope (b) together with standard deviations (SDs) of the regression line for the selected OC and EC concentration data pairs in regional background, suburban area and city centre in all seasons. The slopes represent the $(OC/EC)_P$ ratios.

Site/ Season	Regional background		Suburban area		City centre	
	$a \pm$ SD	$b \pm$ SD	$a \pm$ SD	$b \pm$ SD	$a \pm$ SD	$b \pm$ SD
Autumn	0.71 ± 0.53	3.52 ± 1.11	−0.10 ± 0.27	5.56 ± 0.95	1.06 ± 2.19	2.35 ± 1.77
Winter	0.16 ± 0.09	6.47 ± 0.44	−0.09 ± 0.32	5.43 ± 0.56	0.43 ± 0.29	4.63 ± 0.47
Spring	0.81 ± 0.65	4.40 ± 2.07	0.62 ± 0.008	2.89 ± 0.17	0.85 ± 0.60	1.86 ± 0.69
Summer	1.18 ± 0.16	6.51 ± 1.12	0.86 ± 0.28	3.25 ± 0.53	0.78 ± 0.99	3.60 ± 1.20

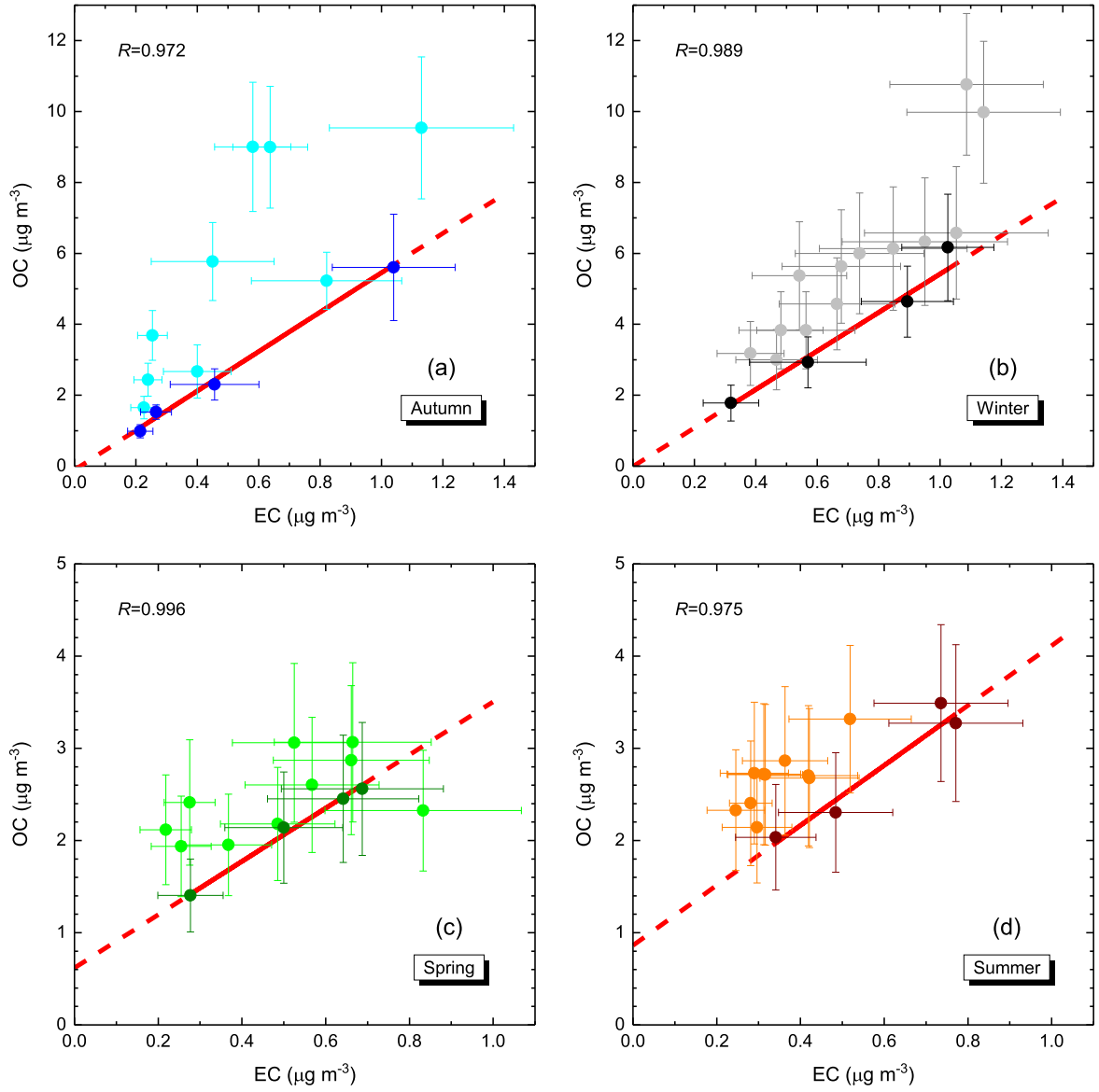

Fig. 1. Scatter plots of organic carbon (OC) and elemental carbon (EC) atmospheric concentrations in the $PM_{2.5}$ size fraction for the suburban area in autumn (a), winter (b), spring (c) and summer (d). In each panel, the symbols in darker shades represent the data that were selected for fitting the linear regression line (in red). The dashed parts of the line are extrapolated. The symbols in lighter shades are the unselected data which are further utilized for estimating the SOC concentrations. The error bars indicate one standard deviation. The coefficient of correlation (R) of the selected data sets is also shown. (For interpretation of the references to colour in this figure legend, the reader is referred to the web version of this article.)

for larger values in winter. They can be explained by the composition of the combustion sources over the year. In spring, FF combustion has larger contributions to TC (by a factor of 3–5) than BB within the whole Carpathian Basin, while it is the opposite (by a factor of 2–3) in winter (Salma et al., 2020). The dependency of the slope of the regression line on the sampling location in autumn and summer was not interpreted because of larger uncertainties of some individual ratios and possibly more complex mixed overall situations as far as the source intensities are concerned. It is worth emphasizing that deriving and adopting seasonally split $(OC/EC)_P$ ratios are both desirable and beneficial for achieving a closer match with the basic assumption of the EC traces method (Sect. 2.2), thus under general environmental conditions which are mostly similar to each other in a daily scale within a season.

There were also substantial differences in the intercepts for the seasons at all sites. They tended to be insignificantly different from zero in autumn and winter. This implies that the production of OC from additional sources than the major combustion emissions [which were accounted for by the $(OC/EC)_P$ ratio] was negligible with respect to these major combustion sources. In spring and summer, however, the intercepts were substantially larger than zero. The intercept is sometimes interpreted as the POC concentration produced from additional processes not involved in the major combustion sources. In our daily samples, this excess amount could be, for instance, the remaining OC concentrations from the previous day(s), which can basically be of both primary and secondary origin. We consider these options as two distinct limiting cases (Sect. 3.2), while the realistic situations most likely occur between them.

3.2. Concentrations

In calculating the SOC concentrations, the intercepts a in Eq. 1 for autumn and winter were regarded to be zero as explained in Sect. 3.1 (see also Fig. 1a and b). For spring and summer, two limiting cases were considered. In the first case, the OC corresponding to the intercept was regarded to be of primary origin ($a > 0$), while in the second case, it was deemed to be of secondary origin ($a = 0$). Based on seasonal tendencies, the second limiting case (OC of the intercept is secondary) yielded more sensible results and the SOC contributions (see later) were internally coherent and laid closer to realistic dependencies inferred indirectly. In contrast, the first limiting case resulted in strange or unlikely seasonal tendencies. In spring and summer, the GRad values and O_3 concentrations are usually much larger than in the other seasons (Salma et al., 2021). This can cause that the OC which persisted from the previous day(s) was already chemically processed in the atmosphere, and, therefore, it can be regarded to be SOC independently of its original source type.

The ranges and medians of SOC concentrations in the regional background, suburban area and city centre were from 0.29 to 4.2 and 1.16 μg m^{-3}; from 0.39 to 5.8 and 1.51 μg m^{-3}; and from 0.54 to 5.2 and 1.42 μg m^{-3}, respectively. The concentrations revealed increasing dependencies from the regional background to the city centre. It is in line with the OC and $PM_{2.5}$ mass tendencies as well. For instance, the annual median OC concentrations were 2.3, 2.9 and 3.3 μg m^{-3}, respectively in the order of the sites listed. Furthermore, atmospheric concentrations are influenced by local meteorological conditions including planetary boundary layer dynamics. This can cause that some chemical species even of different sources vary together in the Carpathian Basin especially under anticyclonic weather situations in winter (Salma et al., 2020). Therefore, it appears to be more informative to evaluate the SOC contributions than atmospheric concentrations.

3.3. Contributions

The annual mean contributions and SDs of the SOC to OC were equally approximately 45% at all sampling locations. They indicated, however, an obvious seasonal dependency. The mean seasonal contributions at each sampling site are summarised in Table 2. The data sets showed a decreasing tendency of the contributions from the regional background through the suburban area to the city centre. This corresponds to our general knowledge on the source types and atmospheric transformation processes of OC.

Table 2
Mean contributions of secondary organic carbon to organic carbon together with standard deviations (SDs; all in %) in the $PM_{2.5}$ size fraction in regional background, suburban area, and city centre in all seasons.

Site/ Season	Regional background		Suburban area		City centre	
	Share	SD	Share	SD	Share	SD
Autumn	59	11	45	18	56	6
Winter	33	7	32	9	22	9
Spring	62	9	49	14	47	6
Summer	66	6	55	9	56	5

In spring and summer, the regional background seemed to be more distinct from the urban sites than the latter two locations from each other. In winter, the regional background and suburban area appeared to resemble themselves more closely than the city centre. This can be explained by similarities and differences in the heating habits and practice. At the regional background and suburban locations, BB is common in winter in contrast to the city centre, where the residential heating is mostly realised through distant heating networks and the intensity of the road vehicle traffic (which produces high abundances of POC) is also larger. Furthermore, in city centres, high concentrations of some specific anthropogenic pollutants such as NO_2 may enhance the formation of SOC from biogenic precursors, and thus, the mechanism is anthropogenically driven (despite the biogenic origin of the precursors; Minguillón et al., 2016; McFiggans et al., 2019). It is noted in this respect that the median NO_2 concentrations in the city centre were larger by a factor of ca. 17 than in the regional background, while the median O_3 concentrations in summer in the city centre was lower by a factor of 1.7 than in the regional background. The former property can be related to more intensive vehicle traffic in cities, while the latter is a result of a large-scale formation mechanism of O_3 typical in the Carpathian Basin.

As far as the seasonal variations at the sites are concerned, the SOC contributions were the smallest in winter. They were approximately of or smaller than 30%. The SOC prevailed in summer. In the regional background, this even reached 66%. The SOC contributions are comparable to or are in line with those for similar European sites (e.g., Castro et al., 1999; Salma et al., 2004; Gelencsér et al., 2007; Minguillón et al., 2016; Daellenbach et al., 2017; Kaskaoutis et al., 2020; Via et al., 2021). Atmospheric concentrations of SOC and their contributions could also be affected by their partitioning between the gas phase and condensed phase, which is temperature dependent. Thus, it could change with season. The mean Ts in autumn, winter, spring and summer at the regional background, suburban area and city centre were 8.4, 10.0 and 12.9; 1.8, 2.5 and 2.5; 17.1, 19.0 and 19.9; and 23, 24 and 24 °C, respectively. They were similar to each other at all sites for each season. The air temperatures in winter could also impact the intensity and type of the residential heating, i.e., the source strength and source composition of the carbonaceous matter and VOCs.

The present values are in line with the SOC contributions for a kerbside site in Budapest in spring 2002 in particular if we consider the larger abundance of the vehicle traffic emissions in such microenvironments. The SOC shares were (37 ± 18)% over daylight periods and (46 ± 16)% over nights (Salma et al., 2004).

Mass concentrations of SOA were roughly estimated from the SOC data by multiplying them with OM/OC mass conversion factor for SOA $[(OM/OC)_{SOA}]$. The factor can show substantial spatial (geographical) and temporal (here seasonal) dependencies, and it is one of the most important causes of uncertainty in chemical mass closure calculations. A relative SD of 30% was estimated for the general OM conversion (Maenhaut et al., 2012). Fulvic acids and atmospheric HULIS are sometimes considered as surrogates for oxidized and chemically aged

OM. The conversion factor for fulvic acids is 1.90 ± 0.02. The mean factors for atmospheric HULIS determined in the same environments as in the present study were 1.9–2.1 (regional background; Kiss et al., 2002) and 1.8 (city centre; Salma et al., 2007). These factors are similar to the mean and SD of 2.1 ± 0.2 proposed for oxidized aerosol (Turpin and Lim, 2001). OM/OC ratios between 1.41 and 2.15 with a mean of 1.71 were derived by AMS for total ambient aerosol in Mexico City in March (Aiken et al., 2008). The data set was subjected to positive matrix factorisation, which resulted in conversion factors for the fresher and more aged SOA of ca. 1.9 and 2.3, respectively. Considering all these and the fact that we deal here with daily samples, an $(OM/OC)_{SOA}$ factor of 1.9 was uniformly adopted at all sites. This selection may somewhat underestimate the SOA from spring to autumn and overestimate it in winter. The contributions obtained are summarised in Table 3.

The contributions mostly represented 20%–25% of the PM mass, except for winter when they were ca. 10%. The mean contributions in each season were fairly similar to each other for all three sites. Except for the city centre, where the shares were formally smaller in winter and possibly larger in summer than at the other two sites. These can partly be explained by the relatively more intense sources of POA in cities in winter and could also be related to the smaller number of samples at this location.

It is worth mentioning that the time intervals with the highest PM mass pollution levels over the year occur almost exclusively in winter. This is related to persistent anticyclonic weather situations and lasting temperature inversions (the so-called cold pillow) above the Carpathian Basin, which restrict the vertical mixing. The lowest contributions of SOA in winter seem to be an advantageous feature from this aspect (assuming more severe health effects of SOA than of PM mass in general). In contrast, PM mass concentrations ordinary exhibit lower levels in summer. The contribution of OC from biogenic sources to TC was shown to be the highest (60%–70%) in this season (Salma et al., 2020), and these particles possess more natural and less harmful chemical composition. Both indices fortunately predict less unfavourable effects of OM and SOA on humans.

3.4. Relationships

The relationships of SOC with the other aerosol constituents, pollutant gases and meteorological properties were investigated. The scatter plots with $PM_{2.5}$ mass, OC, LVG and WSOC at the suburban site and for all seasons are shown in Fig. 2 as examples. The data sets for the other sampling locations were fairly similar to them.

The plots showed obvious dependencies of the SOC on these quantities. In some cases such as $PM_{2.5}$ mass, OC and WSOC, the relationship seemed to be acceptable as a joint dependency for all seasons, while in some other cases, the correlation was maintained only for some seasons. For instance, the SOC correlated with LVG in winter (Fig. 2c), while its correlation with O_3 was significant only in spring and summer. The increase of the $PM_{2.5}$ mass, OC and WSOC on a daily scale could be related with the production of SOC (expressed by the slopes of their regression lines) by factors of approximately 0.14, 0.4 and 0.6, respectively, while the LVG in winter enhanced the SOC by 2.6 times. The observations are consistent with our general ideas on the formation and atmospheric transformation of SOA. They also confirm indirectly the appropriate selection of the data pairs for estimating the $(OC/EC)_P$ ratios (Sect. 3.1).

The scatter plots of SOC on the one side and OC from FF combustion (OC_{FF}), OC from BB (OC_{BB}) and OC from biogenic sources (OC_{Bio}) derived by coupled LVG-radiocarbon method (Salma et al., 2020) and fine-fraction K (as inorganic tracer for BB) on the other side are shown in Fig. S1 in the supplement. These dependences relayed on limited number of data points in each season. They suggested that there was a relationship between the SOC and OC_{FF} in all seasons, between the SOC and OC_{BB} only in winter, and between the SOC and OC_{Bio} in non-winter seasons. They increased the SOC production by factors of approximately 1.4, 0.5 and 1.2, respectively. The Pearson's coefficients of correlation between the SOA and the corresponding mean *T*, WS, RH, EC, NO and CO were not significant.

Table 3
Mean contributions of secondary organic aerosol to $PM_{2.5}$ mass together with standard deviations (SDs; all in %) in regional background, suburban area, and city centre in all seasons.

Site/ Season	Regional background		Suburban area		City centre	
	Share	SD	Share	SD	Share	SD
Autumn	26	6	24	7	21	3
Winter	13	2	13	4	8	3
Spring	29	7	21	5	21	3
Summer	28	5	26	6	32	6

4. Conclusions

Atmospheric concentrations of SOC and its contributions to OC and $PM_{2.5}$ mass were derived using the EC tracer method for POC. The high edge EC approach was adopted to estimate the $(OC/EC)_P$ ratio for the major emission sources. The quantifications were accomplished in three connected continental atmospheric environments, i.e., in a city centre (of Budapest), its suburban area, and its regional background (the Carpathian Basin) in Central Europe in all seasons. The $(OC/EC)_P$ ratios exhibited substantial seasonal and spatial variability from 1.9 to 6.5. The SOC concentrations indicated a decreasing tendency in the order of the locations listed. Their annual mean contributions to OC were approximately 45%. The SOC shares showed a remarkable and substantial seasonal dependency at all sites. The minima (of ca. 30%) occurred in winter, while the maxima with prevailing portions happened in summer. In the regional background, this reached 66%. At all locations, the SOA represented 10% of the $PM_{2.5}$ mass in winter, and it was 25% in the other seasons. These shares, particularly in OC, indicate the important role and consequences of SOA. Furthermore, the conclusions have relevance for the seasonal dependency of the air quality and of the potential adverse health effects of SOA in the Carpathian Basin.

Further insights into SOA could be achieved by adopting evaluation methods with larger time resolution over which atmospheric chemical transformation processes are less advanced. The comparison of the results with different time resolutions from online AMS and offline methods could also be useful and informative since the development of the SOA systems from diverse (precursor) origin may depend differently on their photochemical aging and mixing states.

The assessment of SOC is also essential when considering the role of reactive oxygenated species, which participate in generating inflammatory response from inhalation exposures and which are often related to oxidative stress. The present research results are to be further utilized together with the existing and some new analytical data (e.g., for transition metals and inorganic tracers) in a novel study dedicated to source apportionment of oxidative potential of aerosol particles for the identical atmospheric environments.

Data availability

The observational data are available from the corresponding author.

Author contributions

PTV performed the formal calculations and prepared figures; AM realised most sample collections and the OC/EC analysis; AV accomplished the LVG analysis; IS conceived the research, interpreted the results, and wrote the manuscript with comments from all coauthors.

Financial support

Funding by the Hungarian Research, Development and Innovation

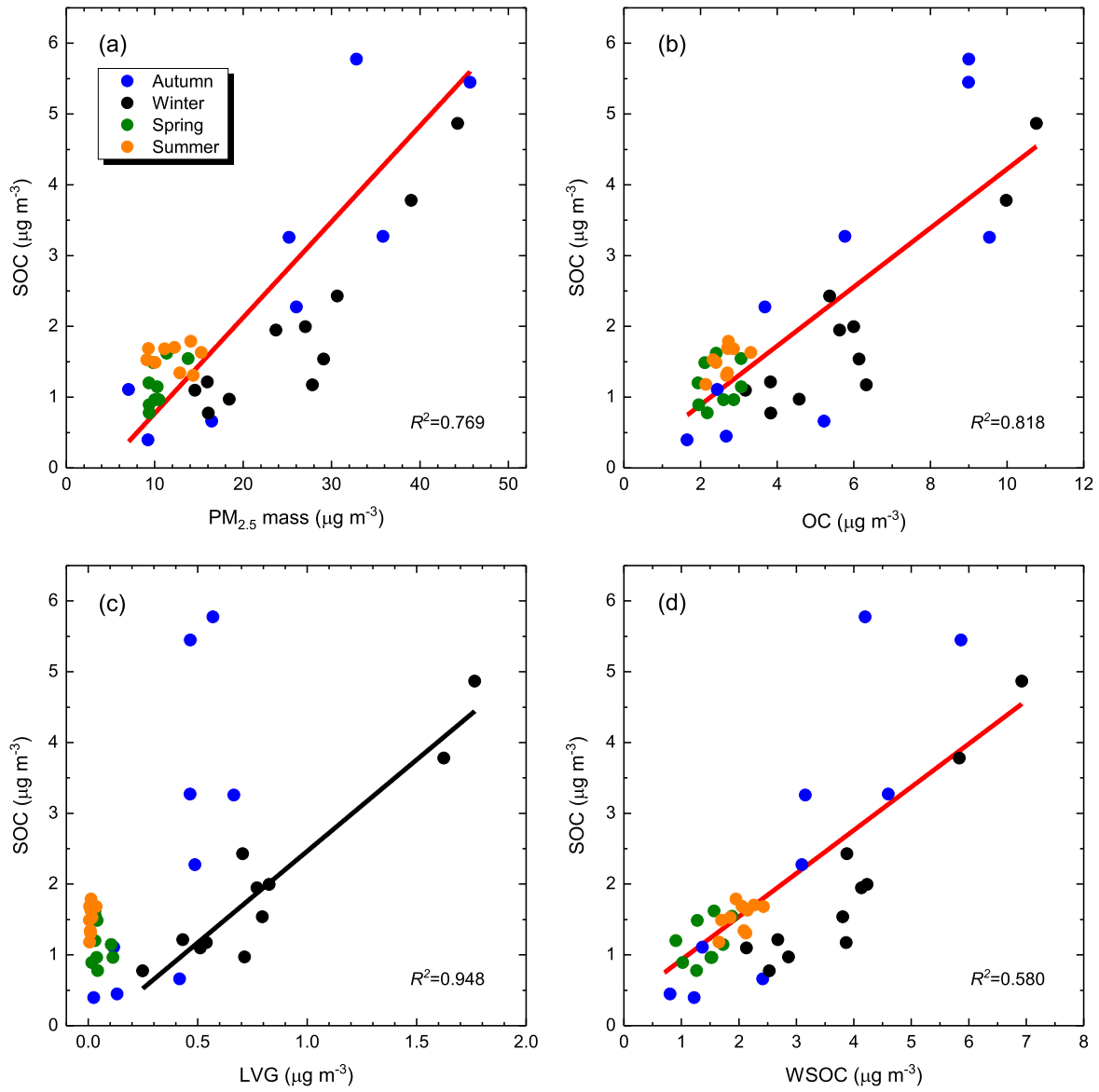

Fig. 2. Scatter plots of secondary organic carbon (SOC) on one side and $PM_{2.5}$ mass (a), organic carbon (OC; b), levoglucosan (LVG; c) and water-soluble organic carbon (WSOC; d) on the other side for the suburban area. The data for each season are indicated in different colours. The fitted linear regression line is displayed in red if it was obtained for all data points and in black if it was derived only for winter. The coefficient of determination (R^2) of the regression is also shown. (For interpretation of the references to colour in this figure legend, the reader is referred to the web version of this article.)

Office (K132254) is acknowledged.

Declaration of Competing Interest

The authors declare that they have no conflict of interest.

Appendix A. Supplementary data

Supplementary data to this article can be found online at https://doi.org/10.1016/j.atmosres.2022.106360.

References

Aiken, A.C., Decarlo, P.F., Kroll, J.H., Worsnop, D.R., Huffman, J.A., Docherty, K.S., Ulbrich, I.M., Mohr, C., Kimmel, J.R., Sueper, D., Sun, Y., Zhang, Q., Trimborn, A., Northway, M., Zeman, P.J., Angarano, M.R., Monarch, T.B., Alfre, M.R., Prevent, A. S.H., Dommer, J., Duplessis, J., Metzger, A., Baltensperger, U., Jimenez, J.L., 2008. O/C and OM/OC ratios of primary, secondary, and ambient organic aerosols with high-resolution time-of-flight aerosol mass spectrometry. Environ. Sci. Technol. 42 https://doi.org/10.1021/es703009q.

Allan, J.D., Delia, A.E., Coe, H., Bower, K.N., Alfarra, M.R., Jimenez, J.L., Middlebrook, A.M., Drewnick, F., Onasch, T.B., Canagaratna, M.R., Jayne, J.T., Worsnopf, D.R., 2004. A generalised method for the extraction of chemically resolved mass spectra from Aerodyne aerosol mass spectrometer data. J. Aerosol Sci. 35, 909–922. https://doi.org/10.1016/j.jaerosci.2004.02.007.

Alves, C.A., Vicente, A.M.P., Gomes, J., Nunes, T., Duarte, M., Bandowe, B.A.M., 2016. Polycyclic aromatic hydrocarbons (PAHs) and their derivatives (oxygenated-PAHs, nitrated-PAHs and azaarenes) in size-fractionated particles emitted in an urban road tunnel. Atmos. Res. 180, 128–137. https://doi.org/10.1016/j.atmosres.2016.05.013.

Blumberger, Z.I., Vasanits-Zsigrai, A., Farkas, G., Salma, I., 2019. Mass size distribution of major monosaccharide anhydrides and mass contribution of biomass burning. Atmos. Res. 220, 1–9. https://doi.org/10.1016/j.atmosres.2019.01.001.

Cabada, J.C., Pandis, S.N., Subramanian, R., Robinson, A.L., Polidori, A., Turpin, B., 2004. Estimating the secondary organic aerosol contribution to $PM_{2.5}$ using, the EC tracer method. Aerosol Sci. Technol. 38, 140e155. https://doi.org/10.1080/02786820390229084.

Carslaw, K.S., Boucher, O., Spracklen, D.V., Mann, G.W., Rae, J.G.L., Woodward, S., Kulmala, M., 2010. A review of natural aerosol interactions and feedbacks within the Earth system. Atmos. Chem. Phys. 10, 1701–1737. https://doi.org/10.5194/acp-10-1701-2010.

Castro, L.M., Pio, C.A., Harrison, R.M., Smith, D.J.T., 1999. Carbonaceous aerosol in urban and rural European atmosphere: estimation of secondary organic carbon

concentrations. Atmos. Environ. 33, 2771–2781. https://doi.org/10.1016/S1352-2310(98)00331-8.
Cavalli, F., Viana, M., Yttri, K.E., Genberg, J., Putaud, J.-P., 2010. Toward a standardised thermal-optical protocol for measuring atmospheric organic and elemental carbon: the EUSAAR protocol. Atmos. Meas. Tech. 3, 79–89. https://doi.org/10.5194/amt-3-79-2010.
Claeys, M., Graham, B., Vas, G., Wang, W., Vermeylen, R., Pashynska, V., Cafmeyer, J., Guyon, P., Andreae, M.O., Artaxo, P., Maenhaut, W., 2004. Formation of secondary organic aerosols through photooxidation of isoprene. Science 303, 1173. https://doi.org/10.1126/SCIENCE.1092805.
Daellenbach, K.R., Stefenelli, G., Bozzetti, C., Vlachou, A., Fermo, P., Gonzalez, R., Piazzalunga, A., Colombi, C., Canonaco, F., Hueglin, C., Kasper-Giebl, A., Jaffrezo, J.-L., Bianchi, F., Slowik, J.G., Baltensperger, U., El-Haddad, I., Prévôt, A.S. H., 2017. Long-term chemical analysis and organic aerosol source apportionment at nine sites in Central Europe: source identification and uncertainty assessment. Atmos. Chem. Phys. 17, 13265–13282. https://doi.org/10.5194/acp-17-13265-2017.
Daellenbach, K.R., Uzu, G., Jiang, J., Cassagnes, L.E., Leni, Z., Vlachou, A., Stefenelli, G., Canonaco, F., Weber, S., Segers, A., Kuenen, J.J.P., Schaap, M., Favez, O., Albinet, A., Aksoyoglu, S., Dommen, J., Baltensperger, U., Geiser, M., El Haddad, I., Jaffrezo, J.L., Prévôt, A.S.H., 2020. Sources of particulate-matter air pollution and its oxidative potential in Europe. Nature 587, 414–419. https://doi.org/10.1038/s41586-020-2902-8.
Day, M.C., Zhang, M., Pandis, S.N., 2015. Evaluation of the ability of the EC tracer method to estimate secondary organic carbon. Atmos. Environ. 112, 317–325. https://doi.org/10.1016/j.atmosenv.2015.04.044.
Ehn, M., Thornton, J.A., Kleist, E., Sipilä, M., Junninen, H., Pullinen, I., Springer, M., Rubach, F., Tillmann, R., Lee, B., Lopez-Hilfiker, F., Andres, S., Acir, I.H., Rissanen, M., Jokinen, T., Schobesberger, S., Kangasluoma, J., Kontkanen, J., Nieminen, T., Kurten, T., Nielsen, L.B., Jorgensen, S., Kjaergaard, H.G., Canagaratna, M., Dal Maso, M., Berndt, T., Petäjä, T., Wahner, A., Kerminen, V.M., Kulmala, M., Worsnop, D.R., Wildt, J., Mentel, T.F., 2014. A large source of low-volatility secondary organic aerosol. Nature 506, 476–479. https://doi.org/10.1038/nature13032.
Fuzzi, S., Baltensperger, U., Carslaw, K., Decesari, S., Denier van der Gon, D.H., Facchini, M.C., Fowler, D., Koren, I., Langford, B., Lohmann, U., Nemitz, E., Pandis, S., Riipinen, I., Rudich, Y., Schaap, M., Slowik, J.G., Spracklen, D.V., Vignati, E., Wild, M., Williams, M., Gilardoni, S., 2015. Particulate matter, air quality and climate: lessons learned and future needs. Atmos. Chem. Phys. 15, 8217–8299. https://doi.org/10.5194/acp-15-8217-2015.
Gelencsér, A., May, B., Simpson, D., Sánchez-Ochoa, A., Kasper-Giebl, A., Puxbaum, H., Caseiro, A., Pio, C., Legrand, M., 2007. Source apportionment of $PM_{2.5}$ organic aerosol over Europe: primary/secondary, natural/anthropogenic, and fossil/biogenic origin. J. Geophys. Res. 112 https://doi.org/10.1029/2006JD008094. D23S04.
Glasius, M., Goldstein, A.H., 2016. Recent discoveries and future challenges in atmospheric organic chemistry. Environ. Sci. Technol. 50, 2754–2764. https://doi.org/10.1021/acs.est.5b05105.
Griffin, R.J., Dabdub, D., Seinfeld, J.H., 2002. Secondary organic aerosol, 1. Atmospheric chemical mechanism for production of molecular constituents. J. Geophys. Res. 107 (D17), 4332. https://doi.org/10.1029/2001JD000541.
Grivas, G., Stavroulas, I., Liakakou, E., Kaskaoutis, D.G., Bougiatioti, A., Paraskevopoulou, D., Gerasopoulos, E., Mihalopoulos, N., 2019. Measuring the spatial variability of black carbon in Athens during wintertime. Air Qual. Atmos. Health 12, 1405–1417. https://doi.org/10.1007/s11869-019-00756-y.
Guenther, A.B., Jiang, X., Heald, C.L., Sakulyanontvittaya, T., Duhl, T., Emmons, L.K., Wang, X., 2012. The model of emissions of gases and aerosols from nature version 2.1 (MEGAN2.1): an extended and updated framework for modeling biogenic emissions. Geosci. Model Dev. 5, 1471–1492. https://doi.org/10.5194/gmd-5-1471-2012.
Hallquist, M., Wenger, J.C., Baltensperger, U., Rudich, Y., Simpson, D., Claeys, M., Dommen, J., Donahue, N.M., George, C., Goldstein, A.H., Hamilton, J.F., Herrmann, H., Hoffmann, T., Iinuma, Y., Jang, M., Jenkin, M.E., Jimenez, J.L., Kiendler-Scharr, A., Maenhaut, W., McFiggans, G., Mentel, Th.F., Monod, A., Prévôt, A.S.H., Seinfeld, J.H., Surratt, J.D., Szmigielski, R., Wildt, J., 2009. The formation, properties and impact of secondary organic aerosol: current and emerging issues. Atmos. Chem. Phys. 9, 5155–5236. https://doi.org/10.5194/acp-9-5155-2009.
Hays, M.D., Smith, N.D., Kinsey, J., Dong, Y., Kariher, P., 2003. Polycyclic aromatic hydrocarbon size distributions in aerosols from appliances of residential wood combustion as determined by direct thermal desorption-GC/MS. J. Aerosol Sci. 34, 1061–1084. https://doi.org/10.1016/S0021-8502(03)00080-6.
Hoyle, C.R., Boy, M., Donahue, N.M., Fry, J.L., Glasius, M., Guenther, A., Hallar, A.G., Huff Hartz, K., Petters, M.D., Petäjä, T., Rosenoern, T., Sullivan, A.P., 2011. A review of the anthropogenic influence on biogenic secondary organic aerosol. Atmos. Chem. Phys. 11, 321–343. https://doi.org/10.5194/acp-11-321-2011.
Jimenez, J.L., Jayne, J.T., Shi, Q., Kolb, C.E., Worsnop, D.R., Yourshaw, I., Seinfeld, J.H., Flagan, R.C., Zhang, X., Smith, K.A., Morris, J.W., Davidovits, P., 2003. Ambient aerosol sampling using the Aerodyne aerosol mass spectrometer. J. Geophys. Res.-Atmos. 108, 8425. https://doi.org/10.1029/2001JD001213.
Jimenez, J.L., Canagaratna, M.R., Donahue, N.M., Prévôt, A.S.H., Zhang, Q., Kroll, J.H., DeCarlo, P.F., Allan, J.D., Coe, H., Ng, N.L., Aiken, A.C., Docherty, K.S., Ulbrich, I. M., Grieshop, A.P., Robinson, A.L., Duplissy, J., Smith, J.D., Wilson, K.R., Lanz, V.A., Hueglin, C., Sun, Y.L., Tian, J., Laaksonen, A., Raatikainen, T., Rautiainen, J., Vaattovaara, P., Ehn, M., Kulmala, M., Tomlinson, J.M., Collins, D.R., Cubison, M.J., Dunlea, E.J., Huffman, J.A., Onasch, T.B., Alfarra, M.R., Williams, P.I., Bower, K., Kondo, Y., Schneider, J., Drewnick, F., Borrmann, S., Weimer, S., Demerjian, K., Salcedo, D., Cottrell, L., Griffin, R., Takami, A., Miyoshi, T., Hatakeyama, S., Shimono, A., Sun, J.Y., Zhang, Y.M., Dzepina, K., Kimmel, J.R., Sueper, D., Jayne, J. T., Herndon, S.C., Trimborn, A.M., Williams, L.R., Wood, E.C., Middlebrook, A.M., Kolb, C.E., Baltensperger, U., Worsnop, D.R., 2009. Evolution of organic aerosols in the atmosphere. Science 326, 1525–1529. https://doi.org/10.1126/science.1180353.
Kanakidou, M., Seinfeld, J.H., Pandis, S.N., Barnes, I., Dentener, F.J., Facchini, M.C., Dingenen, R.V., Ervens, B., Nenes, A., Nielsen, C.J., 2005. Organic aerosol and global climate modelling: a review. Atmos. Chem. Phys. 5, 1053–1123. https://doi.org/10.5194/acp-5-1053-2005.
Kaskaoutis, D.G., Grivas, G., Theodosi, C., Tsagkaraki, M., Paraskevopoulou, D., Stavroulas, I., Liakakou, E., Gkikas, A., Hatzianastassiou, N., Wu, C., Gerasopoulos, E., Mihalopoulos, N., 2020. Carbonaceous aerosols in contrasting atmospheric environments in Greek cities: evaluation of the EC-tracer methods for secondary organic carbon estimation. Atmosphere 11, 161. https://doi.org/10.3390/atmos11020161.
Kiss, G., Varga, B., Galambos, I., Ganszky, I., 2002. Characterization of water-soluble organic matter isolated from atmospheric fine aerosol. J. Geophys. Res. 107 (D21), 8339. https://doi.org/10.1029/2001JD000603.
Kleeman, M.J., Schauer, J.J., Cass, G.R., 2000. Size and composition distribution of fine particulate matter emitted from motor vehicles. Environ. Sci. Technol. 34, 1132–1142. https://doi.org/10.1021/es981276y.
Lanzafame, G.M., Srivastava, D., Favez, O., Bandowe, B.A.M., Shahpoury, P., Lammel, G., Bonnaire, N., Alleman, L.Y., Couvidat, F., Bessagnet, B., Albinet, A., 2021. One-year measurements of secondary organic aerosol (SOA) markers in the Paris region (France): Concentrations, gas/particle partitioning and SOA source apportionment. Sci. Total Environ. 757, 143921 https://doi.org/10.1016/j.scitotenv.2020.143921.
Lelieveld, J., Evans, J.S., Fnais, M., Giannadaki, D., Pozzer, A., 2015. The contribution of outdoor air pollution sources to premature mortality on a global scale. Nature 525, 367–371. https://doi.org/10.1038/nature15371.
Lim, H.J., Turpin, B.J., 2002. Origins of primary and secondary organic aerosol in Atlanta: results of time-resolved measurements during the Atlanta supersite experiment. Environ. Sci. Technol. 36, 4489e4496. https://doi.org/10.1021/es0206487.
Lonati, G., Giugliano, M., Butelli, P., Romele, L., Tardivo, R., 2005. Major chemical components of $PM_{2.5}$ in Milan (Italy). Atmos. Environ. 39, 1925e1934. https://doi.org/10.1016/j.atmosenv.2004.12.012.
Maenhaut, W., Raes, N., Chi, X., Cafmeyer, J., Wang, W., 2008. Chemical composition and mass closure for $PM_{2.5}$ and PM_{10} aerosols at K-puszta, Hungary, in summer 2006. X-Ray Spectrom. 37, 193–197. https://doi.org/10.1002/xrs.1062.
Maenhaut, W., Vermeylen, R., Claeys, M., Vercauteren, J., Matheeussen, C., Roekens, E., 2012. Assessment of the contribution from wood burning to the PM_{10} aerosol in Flanders, Belgium. Sci. Total Environ. 437, 226–236. https://doi.org/10.1016/j.scitotenv.2012.08.015.
McFiggans, G., Mentel, T.F., Wildt, J., Pullinen, I., Kang, S., Kleist, E., Schmitt, S., Springer, M., Tillmann, R., Wu, C., Zhao, D., Hallquist, M., Faxon, C., Le Breton, M., Hallquist, A.M., Simpson, D., Bergstroem, R., Jenkin, M.E., Ehn, M., Thornton, J.A., Alfarra, M.R., Bannan, T.J., Percival, C.J., Priestley, M., Topping, D., Kiendler-Scharr, A., 2019. Secondary organic aerosol reduced by mixture of atmospheric vapours. Nature 565, 587–593. https://doi.org/10.1038/s41586-018-0871-y.
Millet, D.B., Donahue, N.M., Pandis, S.N., Polidori, A., Stanier, C.O., Turpin, B.J., Goldstein, A.H., 2005. Atmospheric volatile organic compound measurements during the Pittsburgh Air Quality Study: Results, interpretation, and quantification of primary and secondary contributions. J. Geophys. Res. 110, D07S07. https://doi.org/10.1029/2004JD004601.
Minguillón, M.C., Pérez, N., Marchand, N., Bertrand, A., Temime-Roussel, B., Agrios, K., Szidat, S., Van Drooge, B., Sylvestre, A., Alastuey, A., Reche, C., Ripoll, A., Marco, E., Grimalt, J.O., Querol, X., 2016. Secondary organic aerosol origin in an urban environment: influence of biogenic and fuel combustion precursors. Faraday Discuss. 189, 337–359. https://doi.org/10.1039/c5fd00182j.
Nault, B.A., Jo, D.S., McDonald, B.C., Campuzano-Jost, P., Day, D.A., Hu, W., Schroder, J.C., Allan, J., Blake, D.R., Canagaratna, M.R., Coe, H., Coggon, M.M., DeCarlo, P.F., Diskin, G.S., Dunmore, R., Flocke, F., Fried, A., Gilman, J.B., Gkatzelis, G., Hamilton, J.F., Hanisco, T.F., Hayes, P.L., Henze, D.K., Hodzic, A., Hopkins, J., Hu, M., Huey, L.G., Jobson, B.T., Kuster, W.C., Lewis, A., Li, M., Liao, J., Nawaz, M.O., Pollack, I.B., Peischl, J., Rappenglück, B., Reeves, C.E., Richter, D., Roberts, J.M., Ryerson, T.B., Shao, M., Sommers, J.M., Walega, J., Warneke, C., Weibring, P., Wolfe, G.M., Young, D.E., Yuan, B., Zhang, Q., de Gouw, J.A., Jimenez, J.L., 2021. Secondary organic aerosols from anthropogenic volatile organic compounds contribute substantially to air pollution mortality. Atmos. Chem. Phys. 21, 11201–11224. https://doi.org/10.5194/acp-21-11201-2021.
Nozière, B., Kalberer, M., Claeys, M., Allan, J., D'Anna, B., Decesari, S., Finessi, E., Glasius, M., Grgić, I., Hamilton, J.F., Hoffmann, T., Iinuma, Y., Jaoui, M., Kahnt, A., Kampf, C.J., Kourtchev, I., Maenhaut, W., Marsden, N., Saarikoski, S., Schnelle-Kreis, J., Surratt, J.D., Szidat, S., Szmigielski, R., Wisthaler, A., 2015. The molecular identification of organic compounds in the atmosphere: state of the art and challenges. Chem. Rev. 115, 3919–3983. https://doi.org/10.1021/cr5003485.
Pandis, S.N., Skyllakou, K., Florou, K., Kostenidou, E., Kaltsonoudis, C., Hasa, E., Presto, A.A., 2016. Urban particulate matter pollution: a tale of five cities. Faraday Discuss. 189, 277–290. https://doi.org/10.1039/c5fd00212e.
Pio, C., Cerqueira, M., Harrison, R.M., Nunes, T., Mirante, F., Alves, C., Oliveira, C., de la Campa, A.S., Artíñano, B., Matos, M., 2011. OC/EC ratio observations in Europe: re-thinking the approach for apportionment between primary and secondary organic carbon. Atmos. Environ. 45, 6121–6132. https://doi.org/10.1016/j.atmosenv.2011.08.045.

Robinson, A.L., Donahue, N.M., Shrivastava, M.K., Weitkamp, E.A., Sage, A.M., Grieshop, A.P., Lane, T.E., Pierce, J.R., Pandis, S.N., 2007. Rethinking organic aerosol: semivolatile emissions and photochemical aging. Science 315, 1133061. https://doi.org/10.1126/science, 1259e1262.

Saleh, R., Marks, M., Heo, J., Adams, P.J., Donahue, N.M., Robinson, A.L., 2015. Contribution of brown carbon and lensing to the direct radiative effect of carbonaceous aerosols from biomass and biofuel burning emissions. J. Geophys. Res. 120 https://doi.org/10.1002/2015JD023697, 10.285–10.296.

Salma, I., Chi, X., Maenhaut, W., 2004. Elemental and organic carbon in urban canyon and background environments in Budapest, Hungary. Atmos. Environ. 38, 27–36. https://doi.org/10.1016/j.atmosenv.2003.09.047.

Salma, I., Ocskay, R., Chi, X., Maenhaut, W., 2007. Sampling artefacts, concentration and chemical composition of fine water-soluble organic carbon and humic-like substances in a continental urban atmospheric environment. Atmos. Environ. 41, 4106–4118. https://doi.org/10.1016/j.atmosenv.2007.01.027.

Salma, I., Németh, Z., Weidinger, T., Kovács, B., Kristóf, G., 2016. Measurement, growth types and shrinkage of newly formed aerosol particles at an urban research platform. Atmos. Chem. Phys. 16, 7837–7851. https://doi.org/10.5194/acp-16-7837-2016.

Salma, I., Németh, Z., Weidinger, T., Maenhaut, W., Claeys, M., Molnár, M., Major, I., Ajtai, T., Utry, N., Bozóki, Z., 2017. Source apportionment of carbonaceous chemical species to fossil fuel combustion, biomass burning and biogenic emissions by a coupled radiocarbon–levoglucosan marker method. Atmos. Chem. Phys. 17, 13767–13781. https://doi.org/10.5194/acp-17-13767-2017.

Salma, I., Vasanits-Zsigrai, A., Machon, A., Varga, T., Major, I., Gergely, V., Molnár, M., 2020. Fossil fuel combustion, biomass burning and biogenic sources of fine carbonaceous aerosol in the Carpathian Basin. Atmos. Chem. Phys. 20, 4295–4312. https://doi.org/10.5194/acp-20-4295-2020.

Salma, I., Thén, W., Aalto, P., Kerminen, V.-M., Kern, A., Barcza, Z., Petäjä, T., Kulmala, M., 2021. Influence of vegetation on occurrence and time distributions of regional new aerosol particle formation and growth. Atmos. Chem. Phys. 21, 2861–2880. https://doi.org/10.5194/acp-21-2861-2021.

Strader, R., Lurman, F., Pandis, S.N., 1999. Evaluation of secondary organic aerosol formation in winter. Atmos. Environ. 33, 4849–4863. https://doi.org/10.1016/S1352-2310(99)00310-6.

Swietlicki, E., Hansson, H.C., Hämeri, K., Svenningsson, B., Massling, A., McFiggans, G., McMurry, P.H., Petäjä, T., Tunved, P., Gysel, M., Topping, D., Weingartner, E., Baltensperger, U., Rissler, J., Wiedensohler, A., Kulmala, M., 2008. Hygroscopic properties of submicrometer atmospheric aerosol particles measured with H-TDMA instruments in various environments – a review. Tellus B 60, 432–469. https://doi.org/10.1111/j.1600-0889.2008.00350.x.

Tang, R., Wu, Z., Li, X., Wang, Y., Shang, D., Xiao, Y., Li, M., Zeng, L., Wu, Z., Hallquist, M., Hu, M., Guo, S., 2018. Primary and secondary organic aerosols in summer 2016 in Beijing. Atmos. Chem. Phys. 18, 4055–4068. https://doi.org/10.5194/acp-18-4055-2018.

Timonen, H., Karjalainen, P., Saukko, E., Saarikoski, S., Aakko-Saksa, P., Simonen, P., Murtonen, T., Dal Maso, M., Kuuluvainen, H., Bloss, M., Ahlberg, E., Svenningsson, B., Pagels, J., Brune, W.H., Keskinen, J., Worsnop, D.R., Hillamo, R., Rönkkö, T., 2017. Influence of fuel ethanol content on primary emissions and secondary aerosol formation potential for a modern flex-fuel gasoline vehicle. Atmos. Chem. Phys. 17, 5311–5329. https://doi.org/10.5194/acp-17-5311-2017.

Tsigaridis, K., Kanakidou, M., 2007. Secondary organic aerosol importance in the future atmosphere. Atmos. Environ. 41, 4682–4692. https://doi.org/10.1016/j.atmosenv.2007.03.045.

Turpin, B.J., Huntzicker, J.J., 1995. Identification of secondary organic aerosol episodes and quantification of primary and secondary organic aerosol concentrations during SCAQS. Atmos. Environ. 23, 3527–3544. https://doi.org/10.1016/1352-2310(94)00276-Q.

Turpin, B.J., Lim, H.-J., 2001. Species contributions to $PM_{2.5}$ mass concentrations: revisiting common assumptions for estimating organic mass. Aerosol Sci. Technol. 35, 602–610. https://doi.org/10.1080/02786820119445.

Via, M., Minguillón, M.C., Reche, C., Querol, X., Alastuey, A., 2021. Increase in secondary organic aerosol in an urban environment. Atmos. Chem. Phys. 21, 8323–8339. https://doi.org/10.5194/acp-21-8323-2021.

Vicente, E.D., Alves, C.A., 2018. An overview of particulate emissions from residential biomass combustion. Atmos. Res. 199, 159–185. https://doi.org/10.1016/j.atmosres.2017.08.027.

Wang, Y., Voliotis, A., Hu, D., Shao, Y., Du, M., Chen, Y., Alfarra, M.R., McFiggans, G., 2021. On the evolution of sub- and super-saturated water uptake of secondary organic aerosol in chamber experiments from mixed precursors. Atmos. Chem. Phys. Discuss. https://doi.org/10.5194/acp-2021-577, in review.

Wu, C., Yu, J.Z., 2016. Determination of primary combustion source organic carbon-to-elemental carbon (OC / EC) ratio using ambient OC and EC measurements: secondary OC-EC correlation minimization method. Atmos. Chem. Phys. 16, 5453–5465. https://doi.org/10.5194/acp-16-5453-2016.

Wu, C., Wu, D., Yu, J.Z., 2019. Estimation and uncertainty analysis of secondary organic carbon using 1 year of hourly organic and elemental carbon data. J. Geophys. Res. 124, 2774–2795. https://doi.org/10.1029/2018JD029290.

Zhang, Q., Jimenez, J.L., Canagaratna, M.R., Allan, J.D., Coe, H., Ulbrich, I., Alfarra, M. R., Takami, A., Middlebrook, A.M., Sun, Y.L., Dzepina, K., Dunlea, E., Docherty, K., DeCarlo, P.F., Salcedo, D., Onasch, T., Jayne, J.T., Miyoshi, T., Shimono, A., Hatakeyama, S., Takegawa, N., Kondo, Y., Schneider, J., Drewnick, F., Borrmann, S., Weimer, S., Demerjian, K., Williams, P., Bower, K., Bahreini, R., Cottrell, L., Griffin, R.J., Rautiainen, J., Sun, J.Y., Zhang, Y.M., Worsnop, D.R., 2007. Ubiquity and dominance of oxygenated species in organic aerosols in anthropogenically-influenced Northern Hemisphere midlatitudes. Geophys. Res. Lett. 34, L13801. https://doi.org/10.1029/2007gl029979.

Zhang, Q., Worsnop, D.R., Canagaratna, M.R., Jimenez, J.L., 2005. Hydrocarbon-like and oxygenated organic aerosols in Pittsburgh: insights into sources and processes of organic aerosols. Atmos. Chem. Phys. 5, 3289–3311. https://doi.org/10.5194/acp-5-3289-2005.

Supplementary material to:

Secondary organic carbon in different atmospheric environments of a continental region and seasons

Imre SALMA[a,*], Péter Tibor VARGA[a], Anikó VASANITS[a], Attila MACHON[b]

[a] Institute of Chemistry, Eötvös Loránd University, Budapest, Hungary
[b] Air Quality Reference Center, Hungarian Meteorological Service, Budapest, Hungary

Table S1. Start and end dates of the sampling periods and number of aerosol samples collected in the regional background of the Carpathian Basin, suburban area and city centre of Budapest.

Site	Month year	October 2017	January 2018	April 2018	July 2018
Regional background	Days	18–31	09–22	17–30	17–30
	Samples	14	14	14	14
Suburban area	Days	18–31	06–22	17–30	17–01*
	Samples	14	17	14	14
City centre	Days	18–27	10–16	17–23	17–23
	Samples	7	7	7	7

* 01 August 2018

* Corresponding author.
E-mail address: salma.imre@ttk.elte.hu (I. Salma).

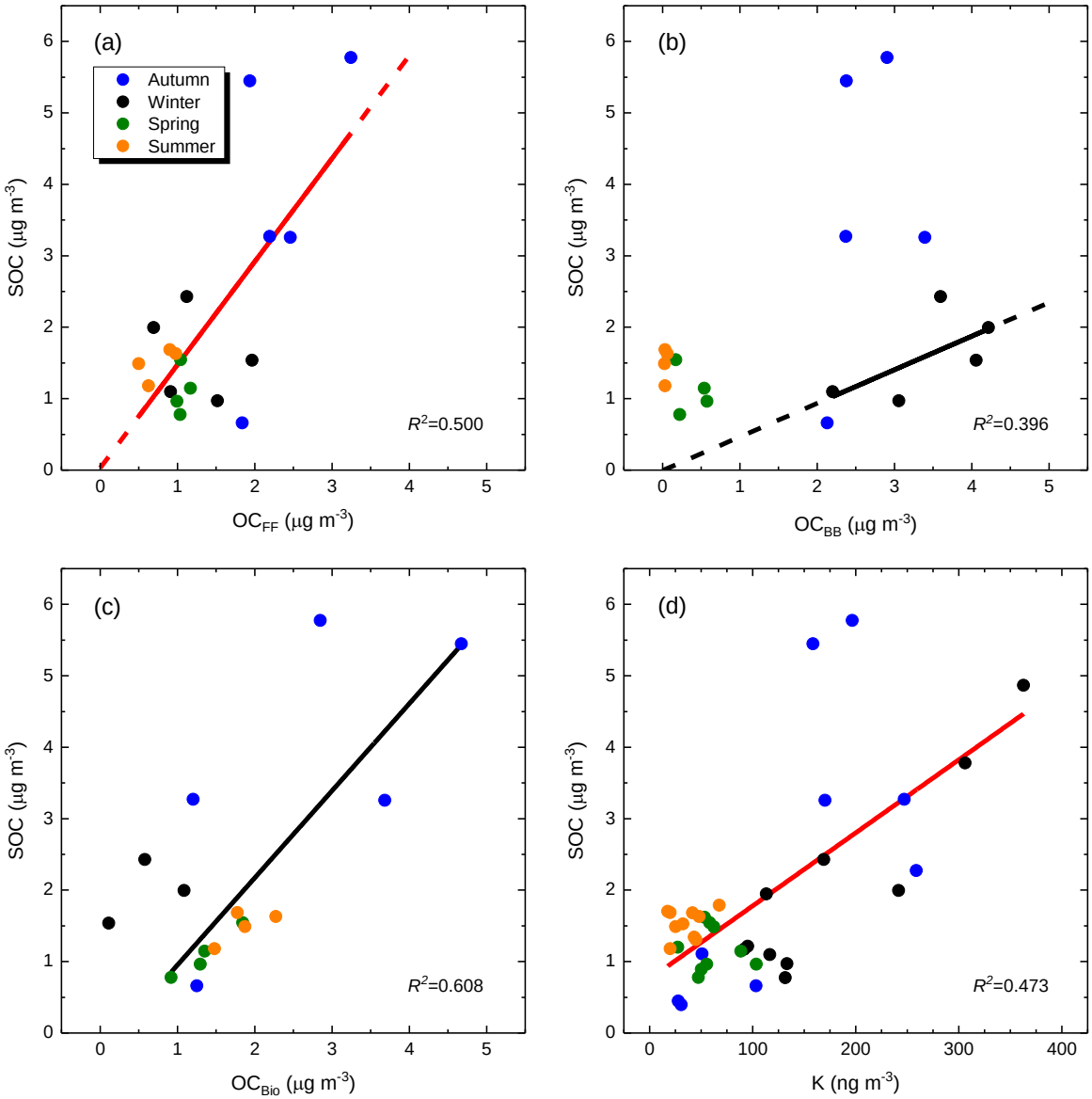

Fig. S1. Scatter plots of secondary organic carbon (SOC) in the $PM_{2.5}$ size faction on the one side and organic carbon (OC) from fossil fuel combustion (OC_{FF}; a), from biomass burning (OC_{BB}; b) and from biogenic sources (OC_{Bio}; c) and K (d) on the other side for the suburban area. The data for each season are indicated in different colours. The fitted linear regression line is displayed in red if it was obtained for all data points and in black if it was derived only for winter (for OC_{BB}; b) or for non-winter seasons (for OC_{Bio}; c). The coefficient of determination (R^2) of the regression is also shown.